

22. FERROMANGANESE AND PHOSPHATIC HARDGROUNDS ON THE WESTERN PACIFIC GUYOTS DRILLED DURING LEGS 143 AND 144¹

Ivar Murdmaa,² Jüri Nemliher,³ Olga Bogdanova,² Anatoli Gorshkov,⁴
Toivo Kallaste,³ and Vera Vasilyeva²

ABSTRACT

Ferromanganese and phosphatic hardgrounds were recovered during Legs 143 and 144 on the Mid-Pacific Mountains and Marshall Islands guyots within the condensed section between the shallow-water carbonate sequence and the pelagic cap on the guyot summits. Ferromanganese oxyhydroxides and phosphates are coupled because of their formation under the same long-term nondepositional environments. Phosphatization was traced downhole to at least 62 mbsf in Hole 867B (Resolution Guyot) within the Albian shallow-water sequence. Mineralogy and geochemistry indicate a hydrogenetic origin of the ferromanganese oxyhydroxides. Phosphates are formed by metasomatic replacement of pelagic and shallow-water biogenic calcite by carbonate-fluorapatite. Uniform composition and lattice structure of the apatite are evidence of equilibrium with normal seawater. Phosphorus for the hardground formation can be supplied from the deep-water reservoir or from the intermediate oxygen-minimum zone. An alternative endo-upwelling model is also discussed.

INTRODUCTION

Ferromanganese crusts and metasomatic phosphates are known to be widespread on the Western Pacific seamounts, particularly on the guyots of the Mid-Pacific Mountains and Marshall Islands. The ferromanganese crusts cover any hard exposed rock surface on the seamount summits and seem to be independent from the substrate composition. Commonly, however, the substrate is represented either by phosphatized limestones (shallow-water or pelagic) or by volcanoclastic rocks (basaltic breccia), which also contain secondary phosphates (e.g., Bezrukov et al., 1969; Hein et al., 1993). Both ferromanganese crusts and phosphates can be interpreted as submarine hardgrounds, formed at the exposed rock surfaces in a long-term nondepositional environment.

Hardgrounds were recovered during Leg 143 at Site 865 (Allison Guyot) as well as Sites 866 and 867 (Resolution Guyot), located in the Mid-Pacific seamounts. During Leg 144, the hardgrounds were drilled on top of three guyots from the Marshall Islands (Limalok, Lo-En, and Wodejebato) and on MIT Guyot near the Mid-Pacific seamounts (see site map preceding title page).

The main purpose of this study is to understand the timing, conditions, and mechanisms of submarine mineralized hardground formation on the Western Pacific guyots in light of new facts recovered during Legs 143 and 144.

METHODS

Lithology and mineralogy of the hardgrounds were investigated using the following methods and equipment.

1. Optical microscopy: description of thin sections and polished sections.

2. Scanning electron microscopy (SEM): study of both natural dry samples and those treated with 6% acidic acid for 20 s to dissolve calcite in phosphatized limestones.

3. Energy dispersive X-ray spectrometry (EDX): study of chemical compositions of apatite, calcite, and ferromanganese oxyhydroxides. Absence of appropriate standards prevented us from calculating element percentages, so only intensities (impulses per second) are given.

4. X-ray diffractometry (XRD): qualitative and semiquantitative determination of phosphates and associated minerals. Shipboard measurements were performed by M.A. Cusimano on the Philips diffractometer, Model PW1710, with CuK α emission. Suspension specimens were primarily used, along with several randomly oriented powder specimens. Semiquantitative apatite content estimates were attempted using a calibration curve obtained from X-ray measurements of artificial apatite/calcite mixtures (0%, 25%, 50%, 75%, and 100% of each constituent).

5. Detailed measurements of the crystallographic and lattice parameters for apatite, calcite, and quartz (in a chert sample) were conducted on the DRON-1.5 diffractometer using randomly oriented powder specimens. A discrete regime was applied with step size 0.002° 2 θ , each point measured every 3 s. Phosphates were investigated within 2 θ intervals at 29°–41° and 57°–64°, which comprise the apatite reflexes (002), (102), (211), (112), (300), (202), (213), (321), (410), and (004). The series of reflex intensities was processed using the distribution equation of Kallaste (1990). The intensity distribution of Gupta and Cullity (1979) was assumed for each reflex. Quartz was used as the standard.

6. We used a transmission electron microscope, Model EM-100, equipped with energy dispersive microprobe Cevex 5100 for precise identification of finely dispersed ferromanganese oxyhydroxide mineral phases. Minerals were determined according to criteria in Chukhrov et al. (1989).

OCCURRENCE AND STRATIGRAPHIC POSITION OF HARDGROUNDS

Phosphatic and ferromanganese oxide mineralizations were detected at all sites drilled during Leg 143 on Allison (Holes 865A and 865B) and Resolution (Holes 866A, 867B, and 868A) guyots. The occurrence of coupled ferromanganese/phosphatic hardgrounds is restricted to the major unconformity between the Albian shallow-water carbonate facies and the Cenozoic pelagic caps, hence marking a carbonate platform drowning event. However, phosphatic hardgrounds also occur within a shallow-water sequence on the Resolution Guyot,

¹ Haggerty, J.A., Premoli Silva, I., Rack, F., and McNutt, M.K. (Eds.), 1995. *Proc. ODP, Sci. Results*, 144: College Station, TX (Ocean Drilling Program).

² Institute of Oceanology, Krasikov St. 23, Moscow 117218, Russian Federation.

³ Institute of Geology, Estonia Ave. 7, Tallinn, Estonia.

⁴ Institute of Geology of Mineral Deposits, Mineralogy and Petrology (IGEM), Staromonetnyi per. 35, Moscow 109017, Russian Federation.

where phosphatized interbeds have been recovered downhole to a depth of 62 mbsf at Site 867 and 319 mbsf in Hole 866A.

Coupled ferromanganese/phosphatic and ferromanganese hardgrounds were drilled during Leg 144 on Limalok, Lo-En, and Wodejebato guyots (Marshall Islands) as well as on MIT Guyot (northwestern Pacific). All of these are related to the condensed section and hiatuses between the top of carbonate platform sequences and the pelagic cap.

At Site 865 (Allison Guyot), fragments of pelagic and shallow-water phosphatized limestones, some having manganese crusts or impregnation, occur between 139.7 and 168.3 mbsf in Cores 143-865A-16R to -20R and Cores 144-865BB-16X to -19X. The actual thickness of the interval is unknown because of the poor core recovery. Many mineralized rock fragments are probably cavings from above, mixed in with in situ shallow-water limestones (Sager, Winterer, Firth, et al., 1993).

The hardground fragments include coupled ferromanganese/phosphatic and single phosphatic varieties. Ferromanganese crusts, as much as 7 cm thick (Sample 143-865A-17R-CC), cover phosphatized and brecciated upper Albian shallow-water carbonates (wackestones, packstones); in some cases, the latter contain cavity infillings of Turonian and Coniacian to Campanian pelagic ooze, which is also phosphatized. A piece of brecciated phosphatic rock cemented and coated by ferromanganese oxyhydroxides was recovered directly below the upper Paleocene foraminifer-nannofossil ooze (Sample 143-865A-16R-CC). A phosphatized shallow-water limestone fragment with Mn-crust in Sample 143-865B-16X-CC was also found just below the base of the upper Paleocene pelagic cap sequence. Some chert fragments have also been found. According to the shipboard thin-section description (Sager, Winterer, Firth, et al., 1993), the cherts contain relicts of sponge spicules and benthic foraminifers, possibly representing a basal facies of the pelagic sequence formed during an initial phase of the carbonate platform drowning.

Syn-sedimentary brecciation and karstification occur throughout the condensed hardground-bearing sequence that spans the time interval between the late Albian (last platform carbonates) and the late Paleocene (beginning of the continuous pelagic sedimentation). The last phosphatization event is fixed in replacement of the Coniacian-Campanian pelagic carbonates; the latter, in turn, indicate a beginning of the carbonate platform drowning. The phosphatization was followed by a ferromanganese oxyhydroxide precipitation during the long-term uppermost Cretaceous to early Paleocene hiatus. Multiple earlier hardground formation events possibly occurred during the Late Cretaceous to form the entire mineralized sequence (Sager, Winterer, Firth, et al., 1993).

At Site 866 (Resolution Guyot), only a few small manganese encrusted and partially phosphatized shallow-water limestone fragments have been recovered in Core 143-866A-3R (10.2–19.6 mbsf) and in Core 143-866B-4M (23.5–32.8 mbsf) below a thin cover of winnowed and reworked pelagic foraminifer ooze, which spans the Maastrichtian to the late Pliocene. These hardground fragments probably represent the mineralized top surface of the Albian shallow-water sequence. A partially phosphatized, yellowish gray wackestone-packstone interbed occurs at 319 mbsf (143-866A-36R-1, 58–59 cm) somewhere below the assumed Aptian/Albian boundary.

Hole 867B, drilled on the north edge of the Resolution Guyot summit, recovered multiple phosphatic hardgrounds in the Albian shallow-water sequence within the depth interval from 0 to 62 mbsf (Cores 143-867B-1R to -9R). In the upper part, the phosphatized rocks are impregnated with Fe-Mn oxyhydroxides. At the top of the hardground-bearing shallow-water sequence, a yellowish brown, Eocene pelagic foraminifer-nannofossil limestone layer several centimeters thick occurs; it is totally phosphatized and impregnated with manganese oxyhydroxide dendrites. The contact between upper Albian floatstone and Eocene foraminifer-nannofossil limestone, representing a long-term hiatus surface, is well preserved in a hardground

specimen (143-867B-1R-1, 0–13 cm; see chapter 8, fig. 3, in Sager, Winterer, Firth, et al., 1993).

The hardground-bearing shallow-water sequence is composed of alternating phosphatized and nonphosphatized beds. The frequency of the phosphatic interbeds is highest in the uppermost part and decreases downward.

Phosphatic mineralization is very weak or absent in Hole 868A, and only local staining by Fe-oxides was observed.

Coupled ferromanganese/phosphatic hardgrounds were drilled during Leg 144 on three guyots of the Marshall Islands: Limalok (Site 871), Lo-En (Site 872), and Wodejebato (Sites 872–877). In Hole 871A (Limalok Guyot), a single small manganese-encrusted phosphatized limestone fragment, with shallow-water limestone pieces (middle Eocene), occurred at 152.9 mbsf. Although the fragment is probably not in place, it apparently represents a hardground from a hiatus surface between the early Miocene pelagic foraminifer ooze above and the underlying middle Eocene benthic foraminifer packstone/wackestone (Premoli Silva, Haggerty, Rack, et al., 1993). This allows us to date the phosphatization event as late Eocene to Oligocene.

On Lo-En Guyot (Site 872), lithostratigraphic Unit II comprises numerous pieces of partially phosphatized pelagic limestone, volcanoclastic sandstone, and conglomerate with volcanoclastic pebbles in phosphatized pelagic limestone. The phosphatized and manganese-encrusted rock fragments represent at least two generations of hardgrounds dated as middle Eocene to late Oligocene and early Campanian to late Paleocene. The condensed hardground-bearing section spans the time interval between late Oligocene foraminifer ooze and Santonian volcanoclastic breccia overlying basalts (Premoli Silva, Haggerty, Rack, et al., 1993).

Hardgrounds from 3 to 14 cm thick were recovered on Wodejebato Guyot (Sites 873, 874, 875, 876, and 877) in the form of phosphate-bearing ferromanganese crusts on top of Maastrichtian platform carbonates. At Site 873, the Mn-encrusted phosphatized limestone fragments occur, mixed with pelagic and neritic limestone pieces, below the early-middle Miocene foraminifer ooze and underlain by the Maastrichtian shallow-water limestone. The phosphatized limestones are dated as middle Eocene to late Paleocene. At other sites, hardgrounds were recovered at the top of a drilled Maastrichtian carbonate platform sequence outcrop; they are dated as early-middle Eocene to late Paleocene (Premoli Silva, Haggerty, Rack, et al., 1993). Therefore, the hardgrounds have been formed between the middle Eocene and early Miocene.

Manganese nodules and crusts were recovered at Site 878 (MIT Guyot) within the condensed pelagic section spanning the time interval from the Santonian-Campanian to the early Eocene, below the late Miocene nannofossil ooze and above the Albian carbonate platform (Premoli Silva, Haggerty, Rack, et al., 1993).

PETROGRAPHY

Ferromanganese oxyhydroxides occur as crusts, fissure infillings, dendrites, and microscopic segregations (spots). A typical ferromanganese crust as thick as 7 cm was recovered in Sample 143-865A-17R-CC. It comprises at least two generations of oxyhydroxide growth. A massive-dendritic inner zone that is about 1 cm thick and has a botryoidal upper surface separates a phosphatized shallow-water detrital limestone (wackestone) from an irregular piece of fine-grained, yellowish brown homogeneous phosphorite, possibly representing a relict of pelagic limestone. This piece (or cavity infilling?) is coated by a thicker outer oxyhydroxide zone. Our SEM study revealed the wavy-laminated dendritic structure of the manganese crust, with a flaky microstructure (Plate 1, Fig. 2).

A piece of brecciated and totally phosphatized pelagic limestone from Sample 143-865A-16R-CC, 12–14 cm, just below the Paleocene nonmineralized foraminifer-nannofossil ooze demonstrates fissure infilling by crystalline apatite and ferromanganese oxyhydroxides. The

fine-grained and rather homogeneous phosphorite is cut by a network of fissures into angular, centimeter-sized fragments. The fissures are filled with elongated prismatic apatite crystals forming millimeter-thick veinlets, which are in turn partially impregnated by ferromanganese oxyhydroxides. The latter penetrate into the thicker veinlets from surficial manganese crust either directly or through a later generation of thin fissures, infilling interstitial space between the apatite crystals. Thus, oxyhydroxide precipitation has apparently been preceded by phosphatization and brecciation. The SEM images show a globular (colloform) microstructure of the ferromanganese oxyhydroxides in fissure infillings (Plate 1, Fig. 1). The ferromanganese crusts from the Leg 144 boreholes are described in Bogdanov et al. (this volume).

Phosphate is developed as a metasomatic replacement of the primary biogenic calcite, either pelagic nannofossil-foraminifer ooze or benthic shallow-water limestones, and as diagenetic cementation leading to infilling of pores and fissures. We have not found any evidence for direct phosphate precipitation during sedimentation, except for the problematic bacterial structures described below. The metasomatic phosphatization displays different structures, starting with thin rims around sparry calcite crystals (Plate 2, Fig. 1) and the dispersal of apatite grains in a micritic carbonate matrix, to the replacement of biomorphic fragments by euhedral apatite crystals (Plate 2, Fig. 2) in microcrystalline apatite/calcite matrix (Plate 2, Fig. 3), and ending the formation of crystalline phosphorite (Plate 1, Figs. 5, 6).

The phosphatized limestones are commonly yellow to yellowish brown and stained by iron oxides. However, no direct correlation can be found between the color shades and the phosphate content, and some strongly phosphatized rocks are very light gray or white as adjacent nonmineralized limestones.

In the partially phosphatized samples, we observed (by SEM) recrystallization of the primary biogenic calcium carbonate. Rhombohedral calcite crystals from 4 to 10 m in size predominate, with minor amounts of large sparry calcite crystals also present. The latter occur as druses in pores or encrust cavity walls. Some calcite crystals are encrusted with phosphatic rims (Plate 2, Fig. 1) likely to have formed simultaneously with calcite recrystallization.

Apatite is represented by a microcrystalline matrix between the euhedral sparry calcite crystals in such samples. Isolated tabular hexagonal crystals also occur, increasing in relative abundance with developing phosphatization, which finally leads to the formation of pure microcrystalline phosphorite composed of tabular hexagonal apatite crystals about 6 m high and 10 m wide. Both patchy and homogeneous distribution of phosphate were observed in phosphatized micritic matrix.

After removal of calcite by acidic acid, casts of calcite crystals appear on the polished surface of the phosphatic matrix (Plate 2, Fig. 4). Within the matrix, isometric bodies (globules) with smooth outer surfaces and radiating crystalline inner structures are visible. Such globules joined together encrust microcavern walls. In the apatitic matrix, fibrous forms also occur (e.g., Sample 143-867B-3R-1, 113–117 cm). These may represent phosphatized relicts of organic filaments, similar to those observed in Holocene guano (Cullen, 1988). We also observed an unidentified branching fibrous network between the euhedral apatite crystals (Sample 143-865A-17R-CC, 5–8 cm; Plate 1, Figs. 3, 4). If not an artifact, this may represent a relict microbial structure.

Rather diverse structural interrelations between the phosphate and ferromanganese oxyhydroxides are demonstrated by an SEM study of the Leg 144 samples. Apatite rims growing on the botryoidal (dendritic) structures of the oxyhydroxides (Bogdanov et al., this volume), as well as microcrystalline apatite segregations (replaced relicts of carbonate sediment?), occur within the ferromanganese crust along with the common metasomatic replacement of biogenic calcium carbonate by apatite before hydrogenetic precipitation of ferromanganese oxyhydroxides. An example of phosphate inclusion is shown on a series of SEM microphotographs (Plate 3).

Table 1. Apatite lattice parameters in phosphatized limestones from Allison and Resolution guyots.

Core, section, interval (cm)	a, Å	c, Å
143-865A-		
16R-CC, 11–12	9.328	6.900
17R-CC, 5–8	9.326	6.900
19R-CC, 9–10	9.328	6.900
20R-CC, 0–1	9.325	6.899
143-865B-		
17X-CC, 46–47	9.327	6.900
143-867B-		
1R-1, 0–1	9.325	6.899
1R-1, 9–13	9.329	6.901
1R-1, 23–25	9.325	6.901
1R-2, 92–94	9.326	6.900
2R-1, 3–5	9.327	6.901
2R-1, 51–52	9.329	6.901
3R-1, 15–17	9.328	6.900
3R-1, 39–41	9.326	6.899
3R-1, 113–117	9.328	6.900
4R-1, 27–30	9.326	6.900

MINERALOGY

The mineralogy of hardgrounds includes the following mineral phases: carbonate-fluorapatite (francolite) and recrystallized Mg-free calcite (in phosphatized limestones), Fe-vernadite, Mn-feroxygite with minor asbolane-buserite, and trace amounts of todorokite (in ferromanganese oxyhydroxides). Chert associated with the hard-ground in Sample 143-865A-17R-CC is composed of quartz.

Apatite XRD patterns are shown on Figure 1, and the lattice parameters are given in Table 1. All samples from Holes 865A and 867B studied in detail demonstrate fairly stable crystallographic and lattice parameters (*a*, *c*) regardless of crystal size and phosphate content in the rock, indicating mineralogical homogeneity of phosphatization.

The low values measured for *a* (Table 1) allow us to identify the phosphate mineral as a carbonate-fluorapatite. The lattice parameters of pure fluorapatite are as follows (Table 2): the replacement of phosphate by carbonate in the fluorapatite lattice, realized in the proportion of 4(CO₃) for 3(PO₄), results in vacant Ca-positions (Nathan, 1984) and lower values of *a*-parameter as compared with pure fluorapatite (McConnell, 1973). The lattice structure of the apatites from the Allison and Resolution guyots differs somewhat from that of common francolite, possibly as a result of the partial replacement of F-positions by Cl-ion. Nevertheless, the low *a*-parameter indicates a high carbonate-ion content, probably close to maximum values for francolite (ca. 6%).

The semiquantitative EDX data reveal positive correlation of Cl, S, Na, and Fe with P in the apatite crystals studied. Figure 2 demonstrates a linear relation between Cl and P intensities (i.e., an increase in chlorine with phosphatization) and an unclear relation between P and S. The low intensity of the chlorine reflex suggests that a few Cl-ions replace F-positions in the lattice. However, common marine francolite contains even less chlorine, so the Cl content in our samples can be responsible for the above-mentioned deviation from the francolite.

All calcites analyzed contain a minor, but persistent, amount of phosphorus and are very low in Mg. However, phosphorus is perhaps not incorporated into the calcite lattice, but forms a separate apatite phase within the newly formed calcite crystals, thus suggesting simultaneous crystallization of both calcite and apatite.

Semiquantitative estimates of the apatite content were made using intensities of main apatite XRD reflexes relative to main calcite peak at 3.04# (Table 3). Sharp changes occur within very short distances in cores (several centimeters or even less), confirming visual impressions about the discrete, not transitional, character of phosphatization. This indicates that phosphatization is associated with certain hard-ground formation events at hiatus surfaces.

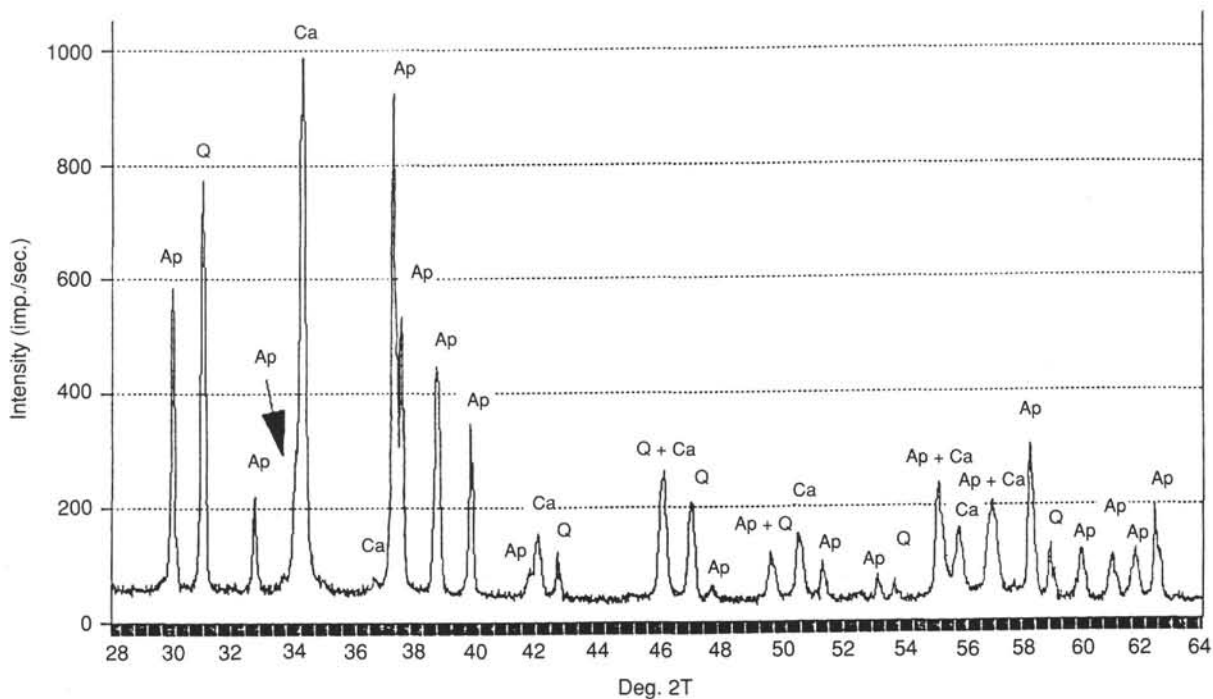


Figure 1. XRD pattern of a phosphatized shallow-water limestone from the Resolution Guyot, Sample 143-867B-3R-1, 113–117 cm. Ap = apatite, Q = quartz (standard), and Ca = calcite.

Table 2. Lattice parameters of pure fluorapatite.

a, Å	c, Å	References
9.3973	6.8782	Hughes et al. (1989)
9.37	6.88	McConnell (1973)
9.364	6.879	Nriagu and Moore (1984)

The mineralogy of ferromanganese oxyhydroxides was studied in two samples from Hole 865A. In Sample 143-865A-17R-CC, 5–8 cm, Fe-vernadite predominates with a minor asbolane-buserite admixture; in a sample from fissure infilling in brecciated and phosphatized limestone (143-865A-16R-CC, 11–12 cm), the dominating mineral is Mn-ferroxigite with a minor admixture of Fe-vernadite and trace amounts of todorokite. Both mineralogies are indicative of hydrogenetic manganese crusts (Bogdanova, 1987).

The chemical composition of the oxyhydroxides (Table 4) is characterized by a low Mn/Fe ratio and Cu content, and a rather high Ni and moderate Co content. Sample 143-865A-17R-CC, 5–8 cm (analyzed by Röhl et al., 1995), contains $\text{Fe}_2\text{O}_3 = 6.65\%$, $\text{MnO} = 11.60\%$, $\text{P}_2\text{O}_5 = 20.53\%$, $\text{Ba} = 0.27\%$, $\text{Cu} = 0.1\%$, $\text{Ni} = 0.36\%$, and $\text{Co} = 0.19\%$.

The chemical data are consistent with a hydrogenic origin of the manganese crusts, as are the results of mineralogical study (Bogdanova, 1987).

DISCUSSION

Drilling on the western Pacific guyots during Legs 143 and 144 recovered two types of submarine mineralized hardgrounds: coupled ferromanganese/phosphatic and single phosphatic.

The coupled hardgrounds are confined solely to the condensed sequence and have repeated long-term hiatuses between shallow-water carbonate platform deposits and the pelagic cap. On the Mid-Pacific guyots (Allison and Resolution) and the MIT Guyot, this disconformity falls into the interval between the Albian and Cenozoic; whereas on the Marshall Islands guyots, this is between the Late Cretaceous (Lo-En, Wodejebato) or Eocene (Limalok) and late Oligocene–early

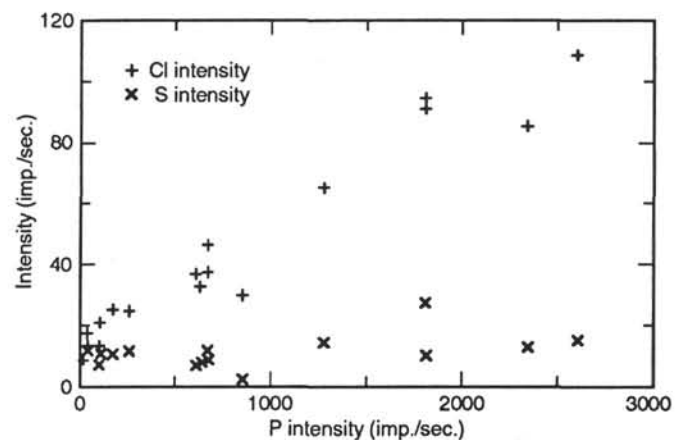


Figure 2. Sulfur and chlorine EDX reflex intensities vs. phosphorus intensities in a sample of partially phosphatized limestone (Sample 143-867B-3R-1, 15–17 cm). Note the almost linear correlation between Cl and P.

Miocene. Assuming that hardgrounds form only at the water-bottom interface, we can infer the age of mineralization from host rock ages (earliest time limit) and from dating of burial events beneath a pelagic cap (latest time limit). The coupled hardgrounds on the Allison Guyot, therefore, were formed during the Late Cretaceous–early Paleocene; those on the MIT Guyot were formed within the time interval between the late Albian and the late Miocene. On the Marshall Islands guyots, a hardground formation is dated before the middle-late Eocene to Oligocene–early Miocene. An earlier (Coniacian–Santonian to early Paleocene) mineralization event is suggested from the dating of hardground fragments on the Lo-En Guyot (Watkins et al., this volume).

The phosphatic hardgrounds were recovered within the carbonate platform deposits on the Resolution Guyot. The first occurrence of phosphatization was fixed in Hole 866A, near the Aptian/Albian boundary, and multiple phosphatized beds occur in the upper Albian

Table 3. Apatite content (relative to calcite) in the phosphatized shallow-water limestones, from Resolution Guyot (semiquantitative XRD data).

Core, section, interval (cm)	Apatite (%)	Color
144-867B-		
1R-1, 4-5	0	White
1R-1, 6-7	17	Yellow
1R-1, 23-25	89	Brown
1R-1, 23-25	79	Yellow
1R-1, 33-34	0	White
1R-2, 92-94	92	Brown clast
1R-2, 112-113	0.3	Light yellowish gray
1R-2, 119-121	0	Light gray
2R-1, 11-12	7	Yellow
2R-1, 40-41	0	White
2R-1, 57-58	95	Brown
2R-1, 111-112	0.7	White
2R-1, 112-123	4	Light yellowish gray
2R-2, 10-11	68	Yellow with brown clasts
2R-2, 50-51	0	Light gray
3R-1, 29-31	21	Yellowish white
3R-1, 39-41	95	Yellow
3R-1, 39-41	98	Brown
3R-1, 93-94	0.8	Light yellowish gray
4R-1, 11-12	0.7	Yellowish gray
4R-1, 18-22	13	Light yellowish gray
4R-1, 27-30	10	White
4R-1, 53-54	0	Light gray
9R-1, 20-21	0	White
9R-1, 20-21	4	Light yellowish gray
11R-1, 83-85	0	Light yellowish gray
12R-1, 62-63	0	White

Note: Estimated using a calibration curve obtained from XRD reflex intensities of artificial apatite/calcite mixtures.

sequence in Hole 867B. Thus, the hardground formation can be dated as late Albian.

Our results confirm a different genesis of the hydrogenetic ferromanganese oxyhydroxides and metasomatic phosphates. We think that these two heterogeneous components occur together in the hardgrounds because of common conditions of long-term nondeposition on the seamount summits.

The ferromanganese crusts display both mineralogical (dominating Fe-vernadite or Mn-ferroxigite) and geochemical (low Mn/Fe ratio and high Ni and Co content) evidence for hydrogenetic origins, although partial reprecipitation and metasomatism are well expressed by dendrites, fissure infillings, and replacement of biomorphic particles. Direct precipitation of the oxyhydroxides from bottom waters at the exposed rock surface has been assumed by most previous investigators for manganese crusts of similar geochemistry and mineralogy dredged from numerous Pacific seamounts (e.g., Halbach and Puteanus, 1984; Bogdanov et al., 1990; Bogdanova, 1987; Skornyakova et al., 1989). Low asbolane-buserite content indicates formation of the crusts under conditions of low biological productivity (Bogdanova, 1987; Bogdanov et al., this volume). The rather unusual presence of todorokite in a fissure infilling (Sample 143-865A-16R-CC) is possibly caused by a long-term diagenetic recrystallization of the Upper Cretaceous Mn-oxyhydroxides in a semi-isolated system buried beneath the Cenozoic pelagic sediment cover.

Many authors (e.g., Halbach and Puteanus, 1984; Bogdanov et al., 1990, this volume) relate the hydrogenetic precipitation of the ferromanganese oxyhydroxides on the guyot summits to an oxygen-poor intermediate water mass (oxygen-minimum zone) enriched in Mn, Co, and other minor elements necessary for manganese crust formation. According to such models, iron is supplied from surface waters transported to the bottom with pelagic carbonates and serves as a sorbent for dissolved Mn. Dissolution of planktonic foraminifers well above the lysocline and carbonate compensation depth should be assumed to realize this mechanism of iron supply to seamount summits. Similar conditions of carbonate dissolution also possibly existed in the mid-Cretaceous ocean, when manganese crusts began to grow at the exposed surfaces of drowned Mid-Pacific carbonate platforms,

Table 4. Chemical composition of ferromanganese oxyhydroxides from the Allison Guyot (atomic adsorption spectrometry).

141-860A-Sample no.	Elements (wt%)					
	Fe	Mn	Cu	Ni	Co	Mn/Fe
143-865A-16R-CC, 11-12	15.00	24.66	0.19	0.69	0.23	1.64
143-865A-17R-CC, 5-8	5.38	12.08	0.11	0.49	0.45	2.24

as the guyots reached the oxygen-minimum zone during progressive subsidence.

The metasomatic phosphates associated with the ferromanganese oxyhydroxides in coupled hardgrounds are identical to those in pure phosphatic hardgrounds intercalated within the upper Albian shallow-water carbonate sequence on Resolution Guyot (Site 867). Analogues of such phosphatic hardgrounds without manganese mineralization are known from the Agulhas Bank off South Africa (Baturin, 1978) and from several other offshore shoals; we dredged similar phosphorites of Paleogene age from the Milwaukee Bank, northern Hawaii Chain (Bezrukov et al., 1969; Baturin, 1978).

Uniformity of the apatite lattice structure and composition, revealed from our data, is evidence for common physical and chemical conditions of the metasomatic phosphatization. The chlorine-bearing carbonate-fluorapatite probably represents a stable final structure, which is in equilibrium with seawater.

Although the phosphatic hardgrounds generally seem to be independent of the shallow-water host rock facies, phosphatization is preferably developed in bioclastic wackestones or packstones, especially if those are syngenetically brecciated. Such facies probably reflect high-energy environments, perhaps leading to formation of short-term hiatuses. Common yellow to brown staining by iron oxides as well as positive correlation between Fe and P in the hardgrounds support the latter assumption and indicate oxygenated conditions during mineralization, unlike phosphate formation in Holocene coastal upwellings (Baturin, 1978; Burnett et al., 1983).

Sources of Phosphorus

Possible phosphorus sources and supplying mechanisms required for metasomatic phosphatization on seamount summits are still under discussion. The following hypotheses of phosphorus supply are discussed.

Phosphorus-rich Bottom Waters

Hein et al. (1993) assume that phosphorus-rich bottom waters serve as direct-reacting solutions for the Cenozoic seamount phosphorites and are derived either from the deep-water reservoir or from the oxygen-depleted intermediate waters (oxygen-minimum zone). However, the phosphorus content necessary for the metasomatic replacement can hardly be achieved without an intermediate mechanism of phosphorus concentration in the reacting solution.

Upwelling

In Holocene coastal upwelling systems, the metasomatic (diagenetic) phosphatization of calcareous sediments leading to phosphatic hardground formation on the outer shelf is maintained by P-rich interstitial waters, which are formed by phosphorus release from organic-rich sediments. The latter accumulate under extremely high biological productivity conditions, stimulated by the upwelling of nutrient-rich waters (Baturin, 1978; Birch, 1980). A similar mechanism, involving the P-rich interstitial waters formed within the organic-rich lagoonal facies, possibly acted on the Resolution and Allison guyots in early stages of the carbonate platform development. This is indicated by recovered organic-rich interbeds, although it seems implausible at the late stage just before atoll drowning, when organic-poor benthic carbonates serve as host rocks for phosphatic hardgrounds. The mechanism is certainly inapplicable to the phosphatization of pelagic carbonates after the atoll drowning.

Endo-upwelling

An alternative mechanism needs to be found if preliminary enrichment in phosphorus of the reacting solution is required to initiate metasomatic replacement of carbonates at the water-bottom interface. So-called "endo-upwelling" (Rongerie and Wauthy, 1990; Rongerie et al., 1994), an upward filtration ("flushing") of interstitial waters through porous carbonate platform deposits within the guyot interior, is one of the possible mechanisms. The presence and rather high intensity of seawater flushing through the Allison and Resolution guyots was shown by Paull et al. (1995), based on strontium-isotope data. The flushing pore fluids can be enriched in phosphorus during filtration through organic-rich sediments in the lower part of the shallow-water sequences. Another possible phosphorus source is from leaching through the volcanic edifice. The secondary alteration of P-enriched alkaline basalts results in partial phosphorus removal (Kurnosov et al., this volume), which perhaps continues even after the basalts have been buried beneath the shallow-water carbonate sequence. Seawater can also be enriched in P before it infiltrates a guyot body if the seamount slopes have been bathed by P-rich deep waters or by oxygen-minimum intermediate waters.

Replacement of both shallow-water and pelagic carbonates takes place at the bottom-water interface that serves as a geochemical barrier between the ascending pore fluids and the bottom waters. Disappearance of the barrier after burial beneath the pelagic cap leads to cessation of the hardground formation.

The model can also explain the rather peculiar difference between the extensively phosphatized sequence in Hole 867B and the non-phosphatized one at Site 868, only 200 m apart on the Resolution Guyot. The former may have been drilled into the ascending pore fluid flux, which was active during Late Cretaceous-early Paleogene time, whereas the latter was affected by direct water exchange with P-poor, open-ocean surface waters.

Structural interrelations among hardground-forming components reveal the following succession of mineralization: primary sedimentation of biogenic calcite, recrystallization and replacement of calcite by carbonate-fluorapatite, precipitation of ferromanganese oxyhydroxides accompanied by partial replacement of the phosphatized substrate, partial reprecipitation of phosphates within the ferromanganese crust, and late diagenetic recrystallization of asbolan-buserite to form todorokite. The stages of mineralization partially overlap each other, but an apparent distinction between the preceding phosphatic metasomatism and following oxyhydroxide precipitation from bottom waters suggests a rather independent character to these processes, which are possibly driven by different factors.

The phosphatization of biogenic carbonates is thought to depend mainly on the phosphorus supply into reacting interstitial solutions at the water-bottom interface to reach concentrations sufficient for the calcite replacement by carbonate-fluorapatite. We think that an endo-upwelling mechanism best explains such a supply. Among possible phosphorus sources, the deep-ocean reservoir seems to be the most universal, although leaching from alkaline basalts or from organic-rich sediments within the seamounts should not be neglected as possible sources.

Certain "episodes of phosphogenesis" are suggested from the age distribution of phosphorites (Cook and McElhiny, 1979; Hein et al., 1993), which possibly reflected changes in the oceanic phosphorus (nutrient) reservoir. The phosphatization events on the guyots discussed here correspond to the worldwide Late Cretaceous maximum of phosphate deposits (Allison and Resolution guyots) and to any of the Cenozoic "episodes" enumerated by Hein et al. (1993) (Marshall Islands guyots).

The formation of ferromanganese oxyhydroxide crusts on guyot summits took place in a pelagic realm below a certain depth level, which today lies somewhere around 500 m. At shallower depths, oxyhydroxide precipitation is likely to be eliminated by active biogenic processes in surface waters. If so, we may assume that the transition

from single-component phosphatic hardgrounds to coupled ferromanganese-phosphatic ones, as observed on Resolution Guyot, marks drowning of the guyot summit below a "critical" depth level necessary for the manganese crust growth. Metasomatic phosphatization took place just before and during the atoll drowning followed by Mn-crust formation in relatively deep-water pelagic environments. A nondepositional environment created by bottom currents is required to maintain both processes, thus serving as a main factor for hardground formation.

CONCLUSIONS

We observed multiple phosphatization events on the Mid-Pacific Mountains and Marshall Islands guyots within the time interval from the late Albian to the middle Miocene. They display quite similar mineralogical and geochemical features and correlate with nondepositional episodes. During carbonate platform drowning, phosphatic hardgrounds partially developed with ferromanganese mineralization. The hydrogenetic ferromanganese oxyhydroxide precipitation is commonly preceded by metasomatic phosphatization of either shallow-water or pelagic calcareous sediments. Along with other factors of phosphate supply for the metasomatism (such as upwelling of deep waters or oxygen-depleted intermediate waters), upward filtration of interstitial waters within the porous shallow-water carbonate sequence on guyots (endo-upwelling) should be taken into account. Long-term nondeposition is the most important factor for hardground formation on the seamount summits.

ACKNOWLEDGMENTS

We are grateful to the reviewers for valuable criticism. We thank the crew of the *JOIDES Resolution*, the shipboard marine specialists, and the shipboard scientific parties of Legs 143 and 144 for the opportunity to obtain materials for this study. We thank the personnel of the analytical laboratories at the P.P. Shirshov Institute of Oceanology, Russian Academy of Sciences, and at the Institute of Geology, Estonian Academy Sciences, for conducting work on our samples. The study was supported by the Russian Fundamental Science Foundation Grant "Warm Biosphere."

REFERENCES*

- Baturin, G.N., 1978. *Phosphorite on the Ocean Floor*: Moscow (Nauka). (in Russian)
- Bezrukov, P.L., Andrushchenko, P.F., Murdmaa, I.O., and Skorniyakova, N.S., 1969. Phosphorites on the ocean floor in the central Pacific. *Dokl. Akad. Nauk SSSR*, 185:192-195. (in Russian)
- Birch, G.F., 1980. A model of penecontemporaneous phosphatization by diagenetic and authigenic mechanisms from the western margin of Southern Africa. In Bentor, Y.K. (Ed.), *Marine Phosphorites: Geochemistry, Occurrence, Genesis*. Spec. Publ.—Soc. Econ. Paleontol. Mineral., 29:79-97.
- Bogdanov, Y.A., Sorochin, O.G., Zonenshain, L.P., Kuptzov, V.M., Lisitzina, N.A., and Podrajanski, A.M., 1990. *Ferromanganese Crust and Nodules of Pacific Seamounts*: Moscow (Nauka). (in Russian)
- Bogdanova, O.Y., 1987. Comparative mineralogical and geochemical study of hydrothermal and sedimentary ferromanganese deposits. *Geology of the Tajura Rift*: Moscow (Nauka), 201-206. (in Russian)
- Burnett, W.C., Roe, K.K., and Piper, D.Z., 1983. Upwelling and phosphorite formation in the ocean. In Suess, E., and Thiede, J. (Eds.), *Coastal Upwelling, Its Sediment Records, Part A: Responses of the Sedimentary Regime to Present Coastal Upwelling*: New York (Plenum), 377-397.
- Chukhrov, F.V., Gorshkov, A.I., and Drits, V.A., 1989. *Hypergenic Manganese Oxides*: Moscow (Nauka). (in Russian)

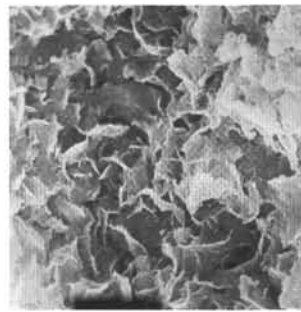
* Abbreviations for names of organizations and publications in ODP reference lists follow the style given in *Chemical Abstracts Service Source Index* (published by American Chemical Society).

- Cook, P.J., and McElhinny, M.W., 1979. A reevaluation of the spatial and temporal distribution of sedimentary phosphate deposits in the light of plate tectonics. *Econ. Geol.*, 74:315–330.
- Cullen, D.J., 1988. Mineralogy of nitrogenous guano on the Bounty Islands, SW Pacific Ocean. *Sedimentology*, 93:421–428.
- Cullen, D.J., and Burnett, W.C., 1986. Phosphorite associations on seamounts in the tropical southwest Pacific Ocean. *Mar. Geol.*, 71:215–236.
- Gupta, S.K., and Cullity, B.D., 1979. Problems associated with K alpha doublet in residual stress measurements. *Adv. X-Ray Anal.*, 23:333–339.
- Halbach, P., and Puteanus, D., 1984. The influence of the carbonate dissolution rate on the growth and composition of Co-rich ferromanganese crusts from Central Pacific seamount areas. *Earth Planet. Sci. Lett.*, 68:73–87.
- Hein, J.R., Yeh, H.-W., Gunn, S.H., Sliter, W.V., Benninger, L.M., and Wang, C.-H., 1993. Two major Cenozoic episodes of phosphogenesis recorded in equatorial Pacific seamount deposits. *Paleoceanography*, 8:293–311.
- Hughes, J.M., Cameron, M., and Crowley, K.D., 1989. Structural variations in natural F, OH and Cl apatites. *Am. Mineral.*, 74:870–876.
- Kallaste, T., 1990. Structural indicators of the origin of Estonian Vendian, Cambrian and Ordovician sedimentary iron sulphides. *Tr.—Akad. Nauk SSSR, Geol. Inst.*, 39:50–59.
- McConnell, D., 1973. *Apatite: Its Crystal Chemistry, Mineralogy, Utilization, and Geologic and Biologic Occurrences*: New York (Springer).
- Nathan, Y., 1984. The mineralogy and geochemistry of phosphorites. In Nriagu, J.O., and Moore, P.B. (Eds.), *Phosphate Minerals: Their Properties and General Modes of Occurrences*: Heidelberg (Springer), 275–291.
- Nriagu, J.O., and Moore, P.B., 1984. Phosphate minerals. In Nriagu, J.O., and Moore, P.B. (Eds.), *Phosphate Minerals: Their Properties and General Modes of Occurrences*: New York (Springer), 8–107.
- Paul, C.K., Fullagar, P.D., Bralower, T.J., and Röhl, U., 1995. Seawater ventilation of Mid-Pacific guyots drilled during Leg 143. In Winterer, E.L., Sager, W.W., Firth, J.V., and Sinton, J.M. (Eds.), *Proc. ODP, Sci. Results*, 143: College Station, TX (Ocean Drilling Program), 231–241.
- Premoli Silva, I., Haggerty, J., Rack, F., et al., 1993. *Proc. ODP, Init. Repts.*, 144: College Station, TX (Ocean Drilling Program).
- Röhl, U., and Strasser, A., 1995. Diagenetic alterations and geochemical trends in Early Cretaceous shallow-water limestones of Allison and Resolution Guyots (Sites 865 to 868). In Winterer, E.L., Sager, W.W., Firth, J.V., and Sinton, J.M. (Eds.), *Proc. ODP, Sci. Results*, 143: College Station, TX (Ocean Drilling Program), 197–229.
- Rougerie, F., Jehl, J., and Trichet, J., 1994. Phosphorus pathways in atolls: endo-upwelling input, microbial accumulation and carbonate-fluorapatite (CFA) precipitation. *Eos*, 75:97.
- Rougerie, F., and Wauthy, B., 1990. Le atoll oasis. *Recherche*, 21:834–842.
- Sager, W.W., Winterer, E.L., Firth, J.V., et al., 1993. *Proc. ODP, Init. Repts.*, 143: College Station, TX (Ocean Drilling Program).
- Skornyakova, N.S., Murdmaa, I.O., and Zaikin, V.N., 1989. Cobalt in ferromanganese crusts and nodules, Pacific Ocean. *Litol. Polezn. Iskop.*, 24:189–202. (in Russian)

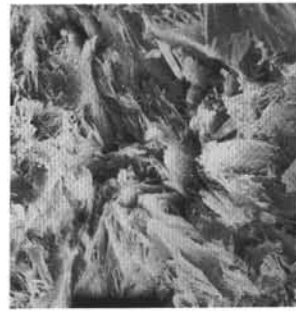
Date of initial receipt: 26 January 1994

Date of acceptance: 28 July 1994

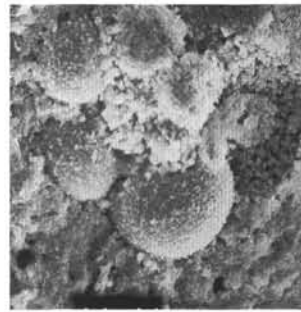
Ms 144SR-070



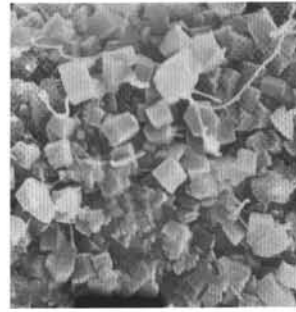
1



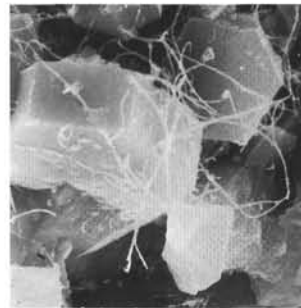
2



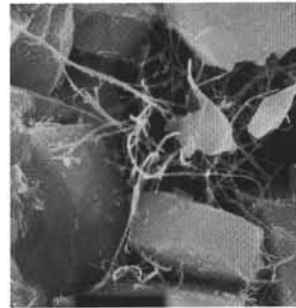
3



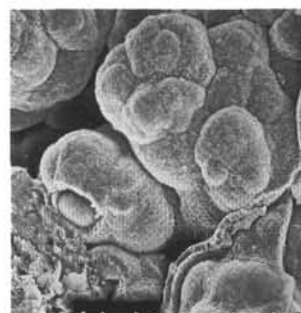
4



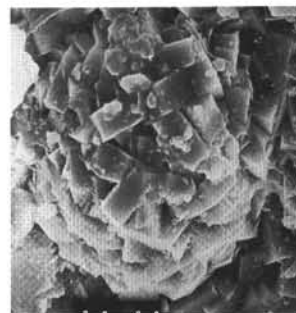
5



6

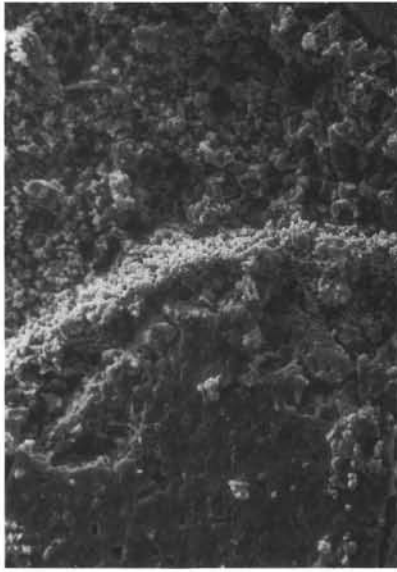


7

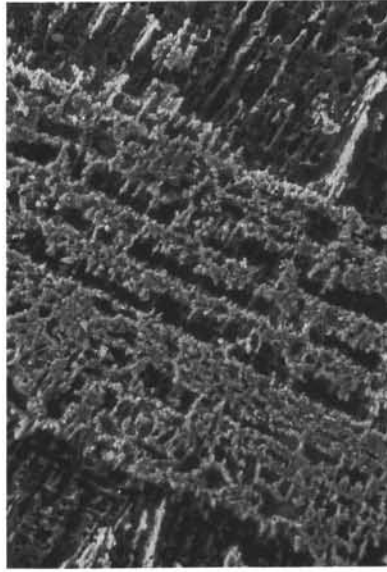


8

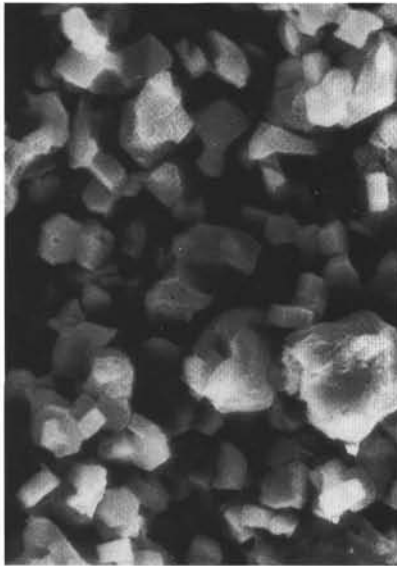
Plate 1. SEM photomicrophotographs of ferromanganese/phosphatic hardgrounds. **1.** Webby, cabbage-like structure of ferromanganese oxyhydroxides indicating early crystallization from gel. Sample 143-865A-16R-CC, 12–14 cm, 2905 \times . **2.** Flaky, ferromanganese oxyhydroxide aggregate from a fissure infilling in crystalline apatite matrix. Sample 143-865A-17R-CC, 5–8 cm, 830 \times . **3.** Phosphatized planktonic foraminifer test in micritic matrix. Sample 143-865A-17R-CC, 5–8 cm, 415 \times . **4.** Fine crystalline apatite from internal wall of foraminifer test shown in Plate 1C, 8300 \times . **5.** Apatite crystals with fibrous net of unknown origin (bacterial?). Sample 143-865A-17R-CC, 5–8 cm, 2490 \times . **6.** Fibrous structure (?) between apatite crystals. The same sample as in Plate 1E, 3320 \times . **7.** Phosphatized planktonic foraminifers. Sample 143-865A-17R-CC, 5–8 cm, 125 \times . **8.** Spheroidal aggregate of crystalline apatite. Sample 143-865B-17X-CC, 46–47 cm, 1245 \times .



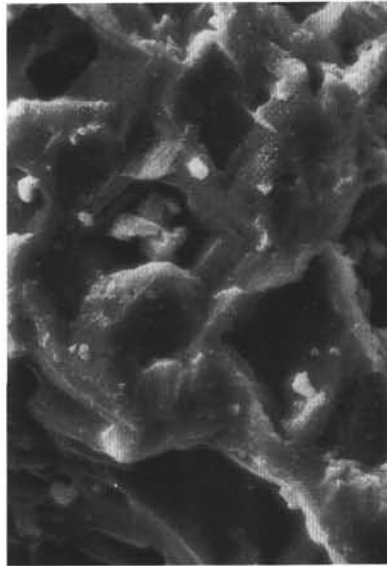
1



2



3



4

Plate 2. SEM photomicrophotographs of phosphatized shallow-water limestones, Hole 867B, Resolution Guyot. Samples were treated with acidic acid. **1.** Slightly phosphatized limestone. Contact between sparry calcite crystal (below) and apatite-containing micritic matrix (above) marked by phosphate rim (white, in central part). Sample 143-867B-3R-1, 113–117 cm, 830 \times . **2.** Slightly phosphatized limestone. Bioclast (shell fragment?) partially replaced by fine crystalline apatite (white, high relief). Sample 143-867B-3R-1, 113–117 cm, 830 \times . **3.** Apatite crystals in phosphatized micritic matrix. Sample 143-867B-3R-1, 15–17 cm, 8300 \times . **4.** Calcite crystals (casts after dissolution) in phosphatic matrix. Sample 143-867B-3R-1, 113–117 cm, 5310 \times .

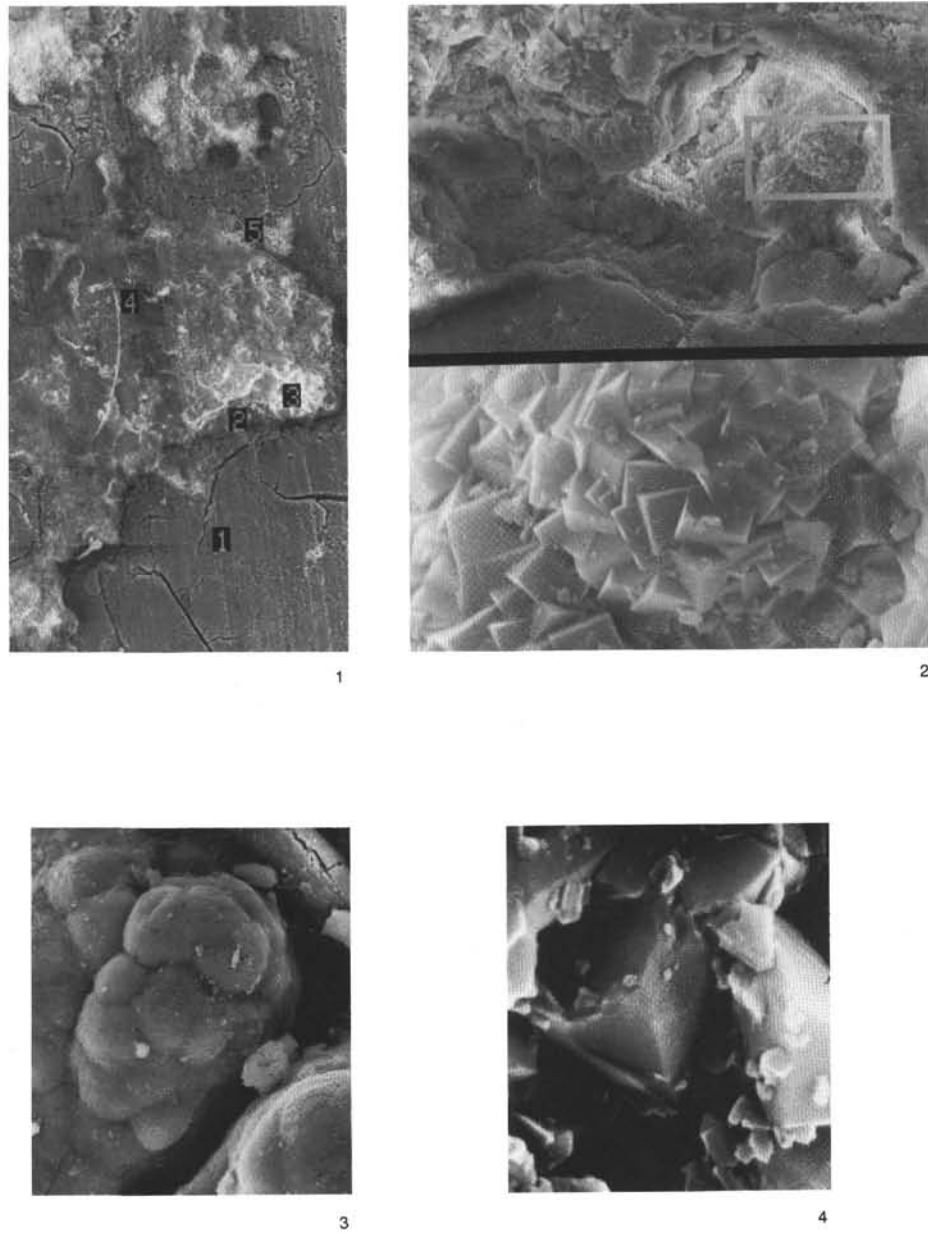


Plate 3. SEM photomicrophotographs of phosphate inclusion (carbonate replaced by phosphate) within Mn-crust. Sample 144-874B-1R-1, 7–10 cm, Wodejebato Guyot. **1.** 1410 \times . **2.** 6640 \times . **3.** 10,790 \times . **4.** 33,200 \times . The numbers on Plate 3A are from EDX microprobe analyses: 1 = Mn-oxyhydroxides; 2, 3, 4, and 5 = phosphate with calcite.